Immunity
Article

The Adaptor Protein MITA Links Virus-Sensing Receptors to IRF3 Transcription Factor Activation

Bo Zhong,[1] Yan Yang,[1] Shu Li,[1] Yan-Yi Wang,[1] Ying Li,[1] Feici Diao,[1] Caoqi Lei,[1] Xiao He,[1] Lu Zhang,[1] Po Tien,[1] and Hong-Bing Shu[1,*]
[1]College of Life Sciences, Wuhan University, Wuhan 430072, China
*Correspondence: shuh@whu.edu.cn
DOI 10.1016/j.immuni.2008.09.003

SUMMARY

Viral infection triggers activation of transcription factors such as NF-κB and IRF3, which collaborate to induce type I interferons (IFNs) and elicit innate antiviral response. Here, we identified MITA as a critical mediator of virus-triggered type I IFN signaling by expression cloning. Overexpression of MITA activated IRF3, whereas knockdown of MITA inhibited virus-triggered activation of IRF3, expression of type I IFNs, and cellular antiviral response. MITA was found to localize to the outer membrane of mitochondria and to be associated with VISA, a mitochondrial protein that acts as an adaptor in virus-triggered signaling. MITA also interacted with IRF3 and recruited the kinase TBK1 to the VISA-associated complex. MITA was phosphorylated by TBK1, which is required for MITA-mediated activation of IRF3. Our results suggest that MITA is a critical mediator of virus-triggered IRF3 activation and IFN expression and further demonstrate the importance of certain mitochondrial proteins in innate antiviral immunity.

INTRODUCTION

Viral infection triggers a series of signaling events that lead to induction of type I interferons (IFNs), including IFN-β and IFN-α family cytokines (Akira et al., 2006; Fitzgerald et al., 2003; Hiscott, 2007; Honda et al., 2006; Katze et al., 2002). Type I IFNs activate the JAK-STAT signal transduction pathways, leading to transcriptional induction of a wide range of genes, such as those that encode IRFs, PKR, IP10, ISGs, and OAS. These downstream gene products mediate inhibition of viral replication and clearance of virus-infected cells, leading to innate antiviral response (Durbin et al., 2000; Levy and Garcia-Sastre, 2001; Levy and Marie, 2004).

Transcriptional induction of type I IFN genes requires the coordinate activation of multiple transcription factors and their cooperative assembly into transcriptional enhancer complexes in vivo. For example, the enhancer of the IFN-β gene contains a κB site recognized by NF-κB, a site for ATF-2-c-Jun, and two IRF-E (also known as PRDIII or ISRE) elements recognized by phosphorylated IRF3 and/or IRF7. It has been shown that transcriptional activation of the IFN-β gene requires coordinate and cooperative assembly of an enhanceosome that contains all of these transcription factors (Honda et al., 2006; Maniatis et al., 1998; Wathelet et al., 1998).

Studies during the past decade have led to breakthrough advances on the virus-triggered type I IFN signaling pathways. The host has developed at least two distinct mechanisms for viral RNA recognition, which represents the first step of innate antiviral response. One is mediated by Toll-like receptors (TLRs), such as TLR3, which recognizes viral dsRNA released by infected cells (Alexopoulou et al., 2001). Engagement of TLR3 by dsRNA triggers TRIF (an adaptor of the TLR pathway)-mediated signaling pathways, thereby leading to IRF3 and NF-κB activation (Han et al., 2004; Oshiumi et al., 2003; Yamamoto et al., 2003; Yamamoto et al., 2002). The second mechanism involves two RNA helicase proteins, RIG-I and MDA5, which function as cytoplasmic viral RNA sensors (Andrejeva et al., 2004; Yoneyama et al., 2004). Both RIG-I and MDA5 contain two CARD modules at their N terminus and a DexD/H-box helicase domain at their C terminus. The helicase domains of RIG-I and MDA5 serve as intracellular viral RNA receptors, whereas the CARD modules are responsible for transmitting signals to downstream CARD-containing adaptor protein VISA (also known as MAVS, IPS-1, and Cardif) (Hornung et al., 2006; Kato et al., 2006; Kawai et al., 2005; Meylan et al., 2005; Pichlmair et al., 2006; Seth et al., 2005; Xu et al., 2005). Gene-deletion studies indicate that VISA is required for the activation of IRF3 and NF-κB, and VISA-deficient mice exhibit severe deficiency in induction of type I IFNs and proinflammatory cytokines and are susceptible to RNA virus infection (Kumar et al., 2006; Sun et al., 2006). Interestingly, the C terminus of VISA contains a transmembrane domain, which targets it to the outer membrane of mitochondria. The mitochondrial localization of VISA is essential for triggering downstream signaling, indicating a critical link between mitochondria and innate antiviral immunity (Seth et al., 2005).

Various studies have demonstrated that the IκB kinase (IKK) family members are critically involved in virus-triggered and VISA-mediated induction of type I IFNs. Although IKKα and IKKβ are essential for virus-triggered NF-κB activation, the noncanonical IKK family members TBK1 and IKKε are responsible for phosphorylating and activating IRF3 and IRF7 (Fitzgerald et al., 2003; Hemmi et al., 2004; Matsui et al., 2006). The mechanisms on how VISA signals the activation of canonical and noncanonical IKK family members, however, are less clear. VISA can interact with tumor necrosis factor (TNF) receptor-associated factor 6 (TRAF6) through its conserved TRAF6-binding motifs. VISA-mediated NF-κB but not IRF3 activation is diminished in TRAF6-deficient fibroblasts, suggesting that TRAF6 acts downstream of VISA in the NF-κB but not IRF3-activation pathway

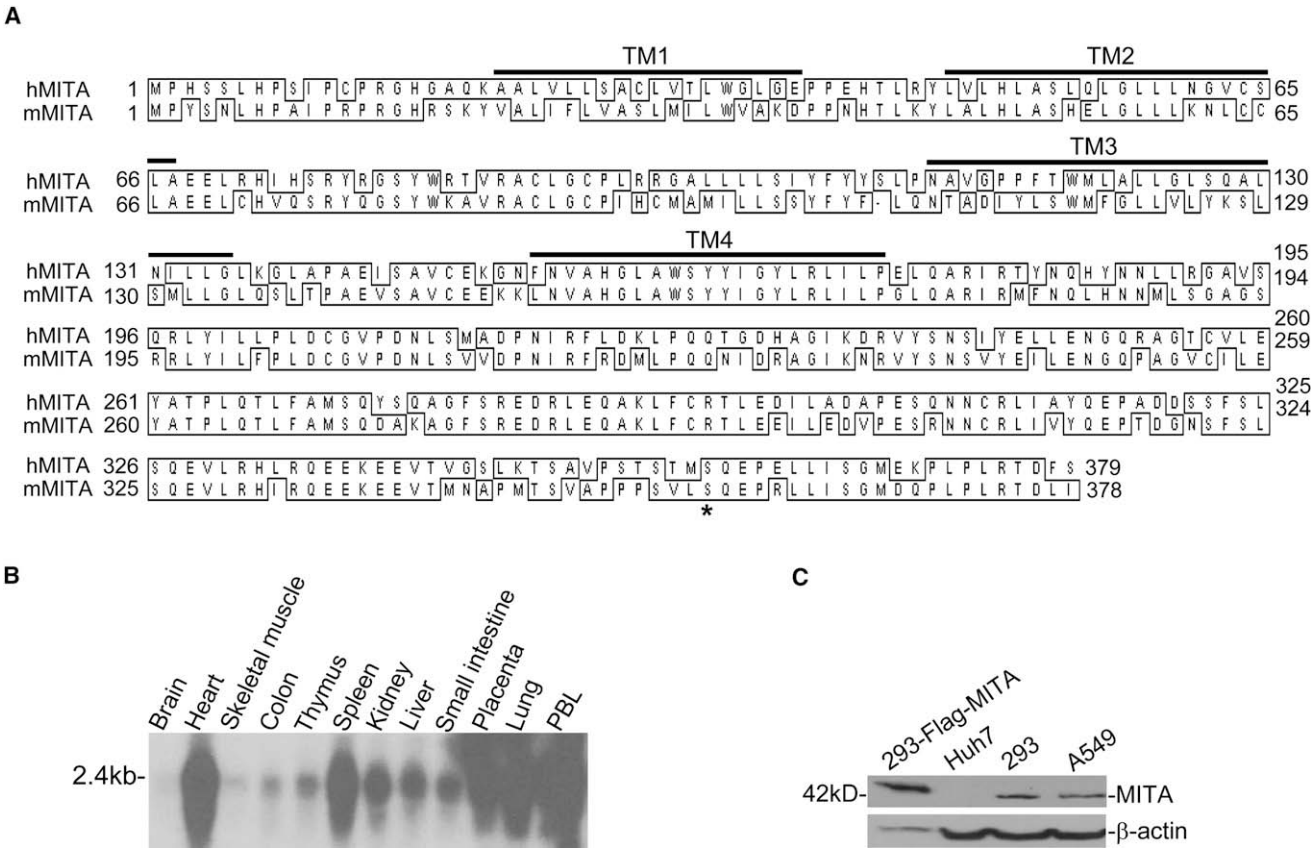

Figure 1. Sequence and Expression Analysis of MITA

(A) Alignment of human and mouse MITA amino acid sequences. Four putative transmembrane regions (TM) are indicated by bold lines. The asterisk marks the serine residue of MITA whose phosphorylation is important for its function.

(B) RNA blot analysis of human MITA mRNA expression.

(C) Immunoblot analysis of human MITA expression in the indicated cell lines. Whole-cell lysates from the indicated cells were analyzed by immunoblotting with a mouse polyclonal antibody against human MITA (aa 221–379). Ten times less lysate was loaded for the Flag-MITA-transfected 293 cell sample. The experiments were repeated for three times with similar results.

(Xu et al., 2005). Other studies indicate that the TNF receptor associated signaling components, including TRADD, FADD, and RIP, interact with VISA and are required for VISA-mediated NF-κB and IRF3 activation (Kawai et al., 2005; Michallet et al., 2008). Gene-deletion studies also suggest a role of TRAF3 in virus-triggered induction of type I IFNs (Oganesyan et al., 2006; Saha et al., 2006).

In this study, we identified an uncharacterized protein, which we designate as MITA. MITA localized to the outer membrane of mitochondria and associated with VISA. MITA acted as an adaptor protein to recruit TBK1 and IRF3 to VISA, and knockdown of MITA abolished virus-triggered IRF3 activation, *IFNB1* expression, and cellular antiviral response. Our findings provide a molecular mechanism on VISA-mediated IRF3-activation pathway and further illustrate the importance of certain mitochondrial proteins in innate antiviral immunity.

RESULTS

Identification of MITA by Expression Cloning

To identify additional proteins involved in virus-triggered IRF3 activation, we performed expression cloning experiments using a reporter construct driven by five copies of IRF-E of the ISG54 gene promoter, which has previously been shown to be activated by IRF3 (Nakaya et al., 2001; Navarro et al., 1998). From ~2×10^5 clones of a human spleen cDNA library screened, we identified seven clones that could activate IRF-E in 293 cells. Sequencing analysis indicated that these clones encode IRF1, IRF3, IRF7, and an uncharacterized protein identified by the NIH full-length cDNA project (GenBank accession number NM_198282). On the basis of its functions described below, we designated this protein as MITA (for *M*ediator of *I*RF3 *A*ctivation). Human MITA contains 379 amino acid residues and shares ~69% sequence identity at the amino acid level with its mouse ortholog (Figure 1A), but has no substantial homology with other proteins. Structural analysis with several programs indicated that MITA contains four putative transmembrane regions but lacks other recognizable motifs or domains (Figure 1A). RNA blot analysis indicated that MITA is ubiquitously expressed as a ~2.4 kb transcript in all examined human tissues (Figure 1B). Immunoblot analysis indicated that MITA is expressed as a 42 kDa protein in human 293 and A549 cells and to a much lower amount in Huh7 cells (Figure 1C and Figure S1 available online).

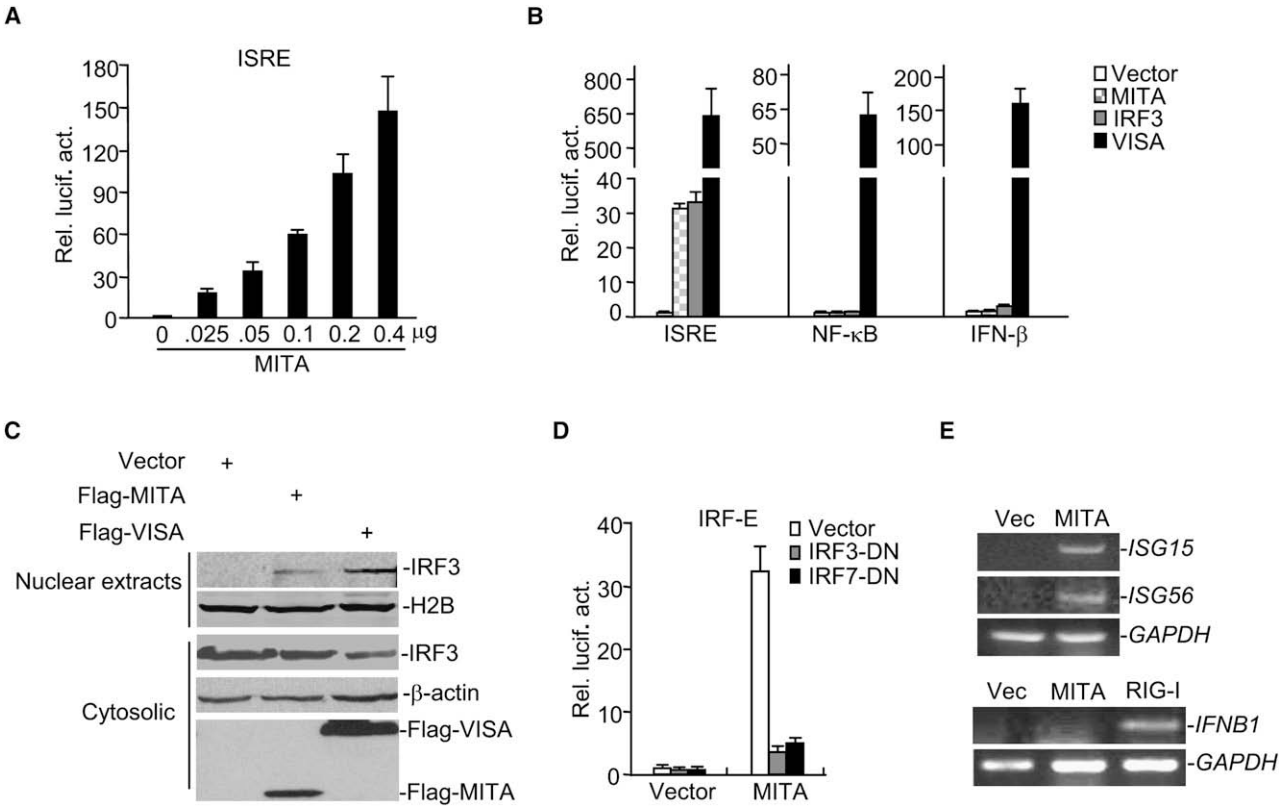

Figure 2. MITA Activates IRF-E but Not NF-κB or IFN-β Promoter

(A) MITA activates IRF-E in a dose-dependent manner in 293 cells. 293 cells (1×10^5) were transfected with IRF-E plasmids (0.1 μg) and the indicated amount of expression plasmid of MITA. Luciferase assays were performed 24 hr after transfection. Graphs show mean ± SD, n = 3.

(B) Comparison of MITA-, IRF3-, and VISA-mediated activation of IRF-E, NF-κB, and the IFN-β promoter. 293 cells (1×10^5) were transfected with the indicated reporter (0.1 μg) and expression (0.1 μg each) plasmids. Luciferase assays were performed 20 hr after transfection. Graphs show mean ± SD, n = 3.

(C) Overexpression of MITA results in IRF3 nuclear translocation. 293 cells (2×10^6) were transfected with the indicated plasmids (8 μg each). About 14 hr after transfection, nuclear extracts (two panels, top) and nonnuclear fractions (three panels, bottom) were prepared and analyzed with the indicated antibodies. The experiments were repeated for three times with similar results.

(D) MITA-mediated IRF-E activation is inhibited by IRF3 and IRF7 mutants. Reporter assays were performed similarly as in (B). Graphs show mean ± SD, n = 3.

(E) Overexpression of MITA induces expression of endogenous *ISG15* and *ISG56* but not *IFNB1* in 293 cells. 293 cells (2×10^5) were transfected with the indicated expression plasmids (2 μg each) for 20 hr before RT-PCR for the indicated genes was performed. The experiments were repeated for three times with similar results.

Overexpression of MITA Activates IRF3

To confirm that MITA is capable of activating IRF-E, we constructed MITA expression plasmids independently of the original clone identified in the expression screens. As shown in Figure 2A, overexpression of MITA activated IRF-E in a dose-dependent manner in 293 cells in reporter assays. The degree of MITA-mediated IRF-E activation was similar to that of IRF3 but markedly lower than that of VISA (Figure 2B), with these proteins expressed at similar amounts (Figure S2). Consistently, overexpression of MITA caused translocation of IRF3 into the nucleus (Figure 2C), whereas MITA-mediated IRF-E activation was inhibited by dominant-negative mutants of IRF3 and IRF7 (Figure 2D). These data suggest that MITA activates IRF-E through IRF3 and IRF7.

Because viral infection also activates NF-κB, we determined whether MITA can activate NF-κB. As shown in Figure 2B, MITA did not activate NF-κB in reporter assays. Consistently, MITA did not activate the IFN-β promoter (Figure 2B), which needs cooperation of NF-κB and IRF3 for activation. Furthermore, overexpression of MITA induced endogenous expression of two IRF-E-dependent antiviral genes *ISG15* and *ISG56* (Nakaya et al., 2001; Wathelet et al., 1987) but failed to induce endogenous expression of *IFNB1* (Figure 2E). These data suggest that overexpression of MITA activates IRF3.

MITA Is Required for Virus-Triggered IRF3 Activation and Cellular Antiviral Response

We next determined whether endogenous MITA is required for virus-triggered IRF3 activation and type I IFN induction. We utilized three MITA-RNAi plasmids that could substantially inhibit the expression of transfected or endogenous MITA (Figure 3A). As shown in Figure 3B, all three MITA-RNAi plasmids potently inhibited Sendai virus (SeV)-induced IRF-E activation (The #2 MITA-RNAi plasmid was used for all the experiments described below. Similar results were obtained with the #1 MITA-RNAi plasmid.). Knockdown of MITA also inhibited SeV-induced

IRF3 dimerization and phosphorylation (Figure 3C), which are hallmarks of IRF3 activation. Although MITA was expressed at a low level in Huh7 cells, it was still required for SeV-induced IRF-E activation in these cells (Figure S3A). Interestingly, although overexpression of MITA did not activate NF-κB, knockdown of MITA inhibited virus-triggered NF-κB activation (Figure 3D), suggesting a potential crosstalk between virus-triggered NF-κB and IRF3-activation pathways at the MITA level. As expected, knockdown of MITA inhibited SeV-triggered activation of the IFN-β promoter (Figure 3E), as well as endogenous expression of *ISG15*, *ISG56*, and *IFNB1* (Figure 3F). In similar experiments, knockdown of MITA did not affect TNF- or IL-1-induced NF-κB activation (Figure 3G). These data suggest that MITA is a critical mediator of virus-triggered activation of IRF3 and expression of *IFNB1* and other IRF3-dependent genes.

Because MITA is critically involved in virus-triggered expression of IRF3-dependent genes, we determined whether MITA plays a role in cellular antiviral response. In plaque assays, overexpression of MITA significantly inhibited VSV replication in a dose-dependent manner in 293 cells ($p < 0.001$), whereas knockdown of MITA had an opposite effect ($p < 0.01$) (Figures 3H and 3I). Similarly, knockdown of MITA also inhibited SeV-induced activation of the IFN-β promoter as well as VSV replication in HeLa cells (Figures S3B and S3C). Collectively, these results suggest that MITA is required for efficient cellular antiviral response.

To determine whether MITA is required for intracellular dsRNA-induced antiviral response, we performed two lines of experiments. In reporter assays, knockdown of MITA inhibited intracellular poly(I:C)-induced IRF-E activation (Figure S4A). Consistently, plaque assays indicated knockdown of MITA inhibited intracellular poly(I:C)-induced antiviral response (Figure S4B). Similarly, knockdown of MITA also inhibited B-DNA-induced activation of IRF-E, NF-κB, and the IFN-β promoter (Figure S4C). These data suggest that MITA is also required for intracellular dsRNA- and B-DNA-induced antiviral response.

MITA Is Localized to the Outer Membrane of Mitochondria

MITA contains multiple putative transmembrane regions and previous studies have shown that VISA is located at the outer membrane of mitochondria (Seth et al., 2005). Therefore, we determined whether MITA is also localized to the mitochondria by cell fractionation and immunoblot analysis (Figure 4A). We found endogenous MITA exclusively existed in the mitochondrial fraction, which also contained VISA and the mitochondrial protein AIF (Figure 4B). MITA was undetectable in other nonmitochondrial fractions, including the endoplasmic reticulum, cytosol, and nucleus (Figure 4B and data not shown). Confocal microscopy indicated that GFP-tagged MITA is colocalized with the mitochondrial stain MitoTracker Red no matter the tag is attached to its N or C terminus (Figure 4C). Deletion analysis indicated that the third transmembrane region (aa 112–135) of MITA was important for its mitochondrial localization (Figure S5). Results from trypsin-protection assays with purified mitochondria indicated that both MITA and VISA were sensitive to trypsin treatment, whereas the mitochondrial inner-membrane protein COX4 was protected (Figure 4D). These data suggest that MITA is localized to the outer membrane of mitochondria.

MITA Interacts with VISA and Is Recruited to RIG-I upon Viral Infection

Because both MITA and VISA are localized to the outer membrane of mitochondria and required for virus-triggered induction of type I IFNs, we determined whether MITA interacts with VISA. Transient transfection and coimmunoprecipitation experiments indicated that MITA interacts with VISA (Figure 5A). Endogenous coimmunoprecipitation experiments indicated that MITA constitutively interacts with VISA in the presence or absence of viral infection (Figure 5B). Previously, it has been demonstrated that a fraction of VISA is redistributed to insoluble fraction after viral infection (Seth et al., 2005). We found that a fraction of MITA is also redistributed to insoluble fraction after SeV infection (Figure S6). These observations suggest that VISA-MITA-mediated signaling may be initiated from the insoluble fraction.

Domain-mapping experiments indicated that the C terminus of VISA (aa 360–540) and the region spanning the third and fourth transmembrane domains of MITA (aa 111–160) were required for their interaction (Figure 5C). Interestingly, the C-terminal fragment of VISA contained the transmembrane domain (Seth et al., 2005) and was sufficient for IRF-E activation (Xu et al., 2005), whereas aa 111–160 of MITA was important for its mitochondrial localization and oligomerization (Figures S5 and S7). In reporter assays, knockdown of VISA by RNAi inhibited RIG-I- but not MITA-mediated IRF-E activation (Figure 5D), whereas knockdown of MITA inhibited VISA- but not TRIF- and TBK1-mediated IRF-E activation (Figure 5E). These data suggest that VISA signals IRF-E activation through MITA.

VISA is an adaptor for signaling triggered by the viral RNA sensor RIG-I. We determined whether MITA is associated with RIG-I through VISA. In mammalian overexpression system, RIG-I interacted with MITA weakly, probably through endogenous VISA. This interaction was enhanced by ectopically expressed VISA (Figure 5F). In untransfected cells, endogenous RIG-I interacted with MITA in viral-infection-dependent manner, and this interaction was diminished by knockdown of VISA (Figure 5G). Consistently, we found that a small fraction of RIG-I is localized to mitochondria upon viral infection (Figure 4B). These data suggest that RIG-I is recruited to the VISA-MITA complex on the mitochondria upon viral infection.

MITA Links IRF3 and TBK1 to VISA

Previous studies have demonstrated that various proteins are involved in VISA-mediated IRF3 and IRF7 activation, including TBK1, IKKε, TRAF3, TRADD, FADD, and RIP. In addition, it has been suggested that VISA induces IRF3 activation through TBK1 in most cell types and IKKε under certain conditions (Hemmi et al., 2004). In transient transfection and coimmunoprecipitation experiments, MITA interacted with TBK1, IKKε, IRF3, and IRF7 but not with IKKα or IRF9 (Figure 6A). MITA also interacted with TRAF3 but not with TRADD, FADD, and RIP (Figure S7 and data not shown). Interestingly, endogenous coimmunoprecipitation experiments indicated that MITA constitutively interacted with IRF3, and this interaction was slightly enhanced after viral infection, although its interaction with TBK1 was viral-infection-dependent in untransfected cells (Figure 6B). Consistently, we found that a fraction of IRF3 was constitutively localized to the mitochondria, whereas a fraction of TBK1 was recruited to the mitochondria upon viral infection (Figure 4B). In

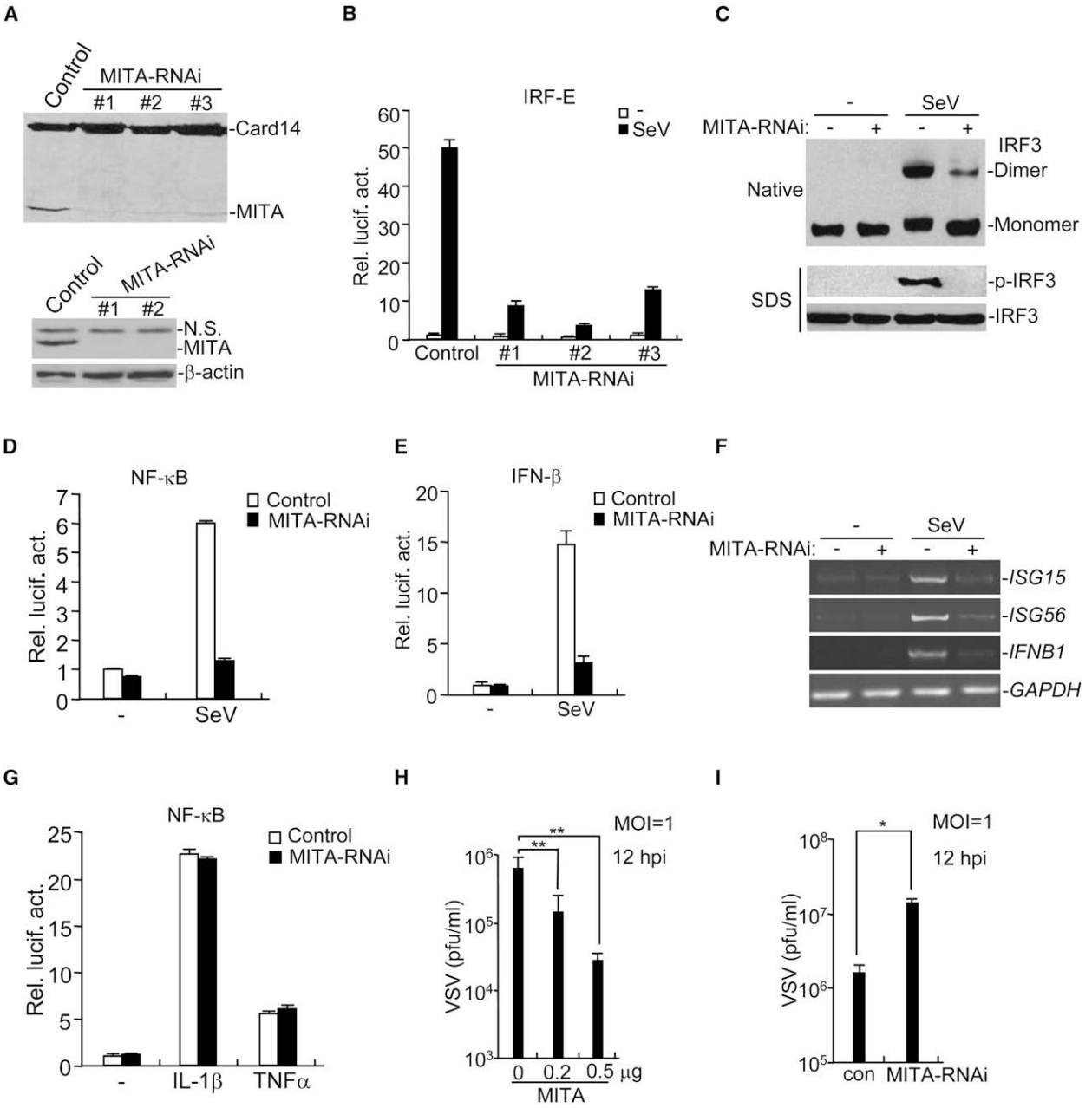

Figure 3. MITA Is Required for Virus-Induced Signaling

(A) Effects of MITA RNAi plasmids on the expression of transfected and endogenous MITA. In the upper panel, 293 cells (1×10^5) were transfected with expression plasmids for Flag-MITA and Flag-CARD14 (0.1 μg each), and the indicated RNAi plasmids (1 μg). At 24 hr after transfection, cell lysates were analyzed by immunoblotting with anti-Flag. In the lower panels, 293 cells (2×10^5) were transfected with control or MITA RNAi plasmids (2 μg each) for 24 hr. Cell lysates were then analyzed by immunoblotting with the indicated antibodies. The experiments were repeated for three times with similar results.

(B) Effects of MITA RNAi plasmids on SeV-induced IRF-E activation. 293 cells (1×10^5) were transfected with the indicated RNAi plasmids. Twenty-four hours after transfection, cells were left uninfected or infected with SeV for 8 hr before luciferase assays were performed. Graphs show mean ± SD, n = 3.

(C) Knockdown of MITA inhibits SeV-induced IRF3 activation. 293 cells (2×10^5) were transfected with a control or MITA RNAi plasmid. Twelve hours after transfection, cells were selected with puromycin (1 μg/ml) for 24 hr, then infected with SeV or left uninfected for 6 hr. Cell lysates were separated by native (upper panel) or SDS (bottom-two panels) PAGE and analyzed with the indicated antibodies. The experiments were repeated for three times with similar results.

(D and E) Effects of MITA RNAi on SeV-induced (D) NF-κB and (E) IFN-β promoter activation. Reporter assays were performed similarly as in (B). Graphs show mean ± SD, n = 3.

(F) MITA RNAi inhibits SeV-induced expression of downstream genes. 293 cells (2×10^5) were transfected with a control or MITA RNAi plasmid (2 μg) for 24 hr RT-PCR was performed 10 hr after SeV infection. The experiments were repeated for three times with similar results.

(G) MITA RNAi does not inhibit TNF- or IL-1-induced NF-κB activation. 293 cells (1×10^5) were transfected with NF-κB reporter plasmid (0.1 μg) together with a control or MITA RNAi plasmid (1 μg each). Twenty-four hours after transfection, cells were left untreated or treated with TNFα or IL-1β (20 ng/ml) for 8 hr before luciferase assays were performed. Graphs show mean ± SD, n = 3.

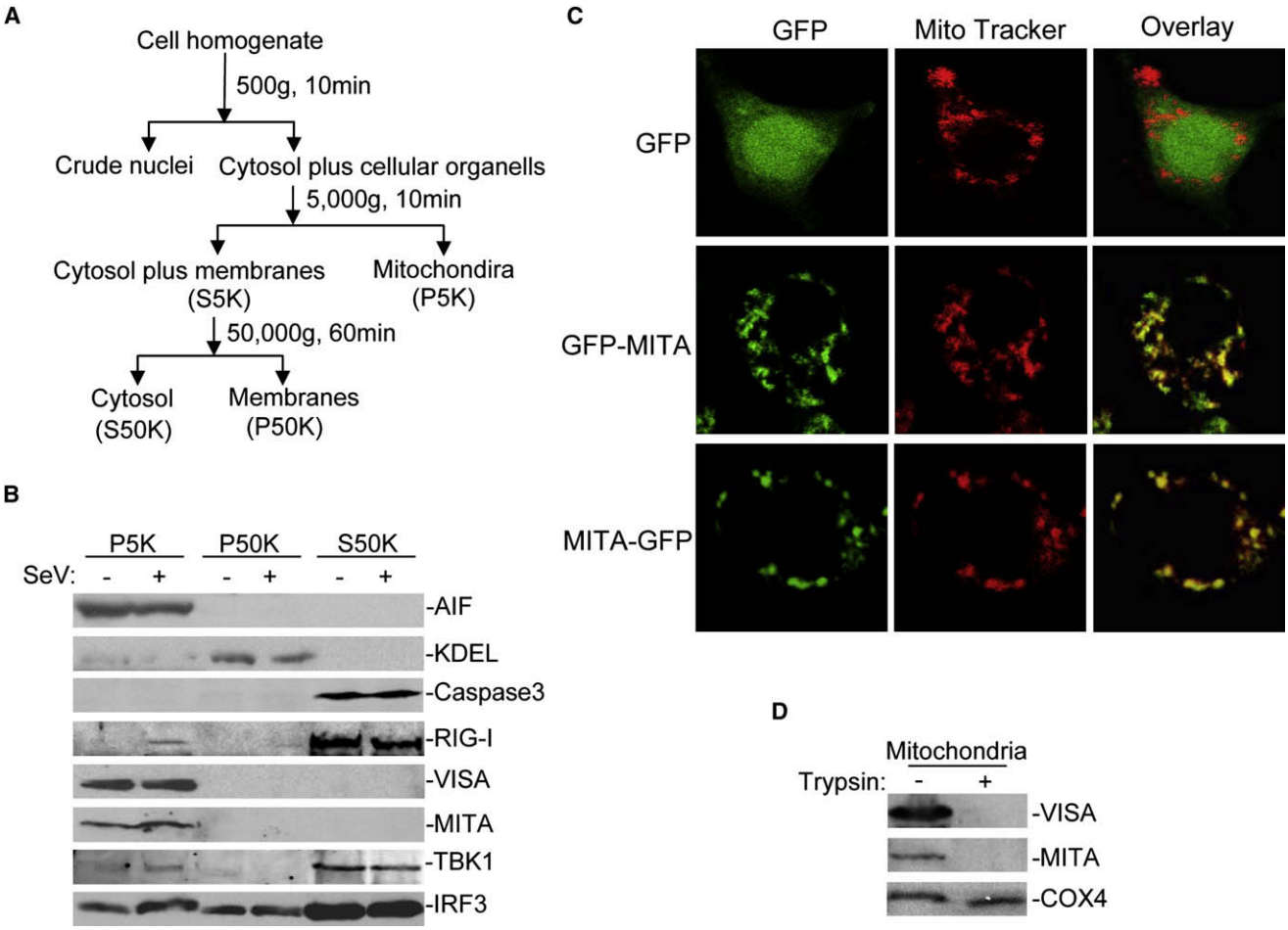

Figure 4. MITA Is Localized to the Outer Membrane of Mitochondria

(A and B) Cell fractionation and immunoblot analysis of the subcellular fractions. Cell fractionation strategy is shown in (A). 293 cells were infected with SeV or left uninfected for 2 hr and cell fractions were analyzed by immunoblotting with the indicated antibodies (B). The experiments were repeated for three times with similar results.

(C) Confocal microscopy of the cellular localization of MITA. 293 cells were transfected with GFP control, N-terminal (GFP-MITA), or C-terminal (MITA-GFP) GFP-tagged MITA. Transfected cells were stained with the MitoTracker Red and observed by confocal microscopy.

(D) MITA is sensitive to trypsin treatment. The purified mitochondria were treated with trypsin (5 μM) or left untreated and then analyzed by immunoblotting with the indicated antibodies. The experiments were repeated for three times with similar results.

addition, phosphorylated IRF3 was also detected in the mitochondrial fraction upon viral infection (Figure S8).

To determine whether MITA is required for recruitment of TBK1 and IRF3 to VISA, we determined the effects of MITA knockdown on the association of VISA with TBK1 and IRF3. Coimmunoprecipitation experiments indicated that knockdown of MITA impaired SeV-induced association of VISA with TBK1 and IRF3 (Figure 6B). These data suggest that TBK1 and IRF3 are linked to the VISA complex through MITA.

We further determined whether MITA can act as a scaffold protein for TBK1 and IRF3. We found that MITA markedly enhanced the interaction between TBK1 and IRF3 in coimmunoprecipitation experiments (Figure 6C). Similarly, MITA also markedly enhanced the interaction between IKKε and IRF3 (Figure S9). Further analysis indicated that MITA could dimerize or oligomerize, depending on its aa 111–160 fragment spanning the last two putative transmembrane regions (Figure S10). Deletion analysis indicated that aa 81–379 of MITA is important for its interaction with TBK1 and IRF3, as well as for enhancing the interaction between TBK1 and IRF3 (Figure S11). Consistently, this fragment was sufficient for activating IRF-E (Figure 6D). These data suggest that MITA acts as a scaffold protein for TBK1 and IRF3 and for linking them to the VISA complex upon viral infection.

(H and I) Effects of MITA on cellular antiviral responses. (H) shows that overexpression of MITA inhibits VSV replication. 293 cells (1×10^5) were transfected with the indicated amount of MITA expression plasmids. At 24 hr after transfection, cells were infected with VSV (MOI = 1) and supernatants were harvested at 12 hr postinfection (hpi). Supernatants were analyzed for VSV production with standard plaque assays. (I) shows that knockdown of MITA increases VSV replication. Plaque assays were performed as in (H), except that MITA RNAi plasmid (1 μg) was used (**$p < 0.001$; *$p < 0.01$). Graphs show mean ± SD, n = 3.

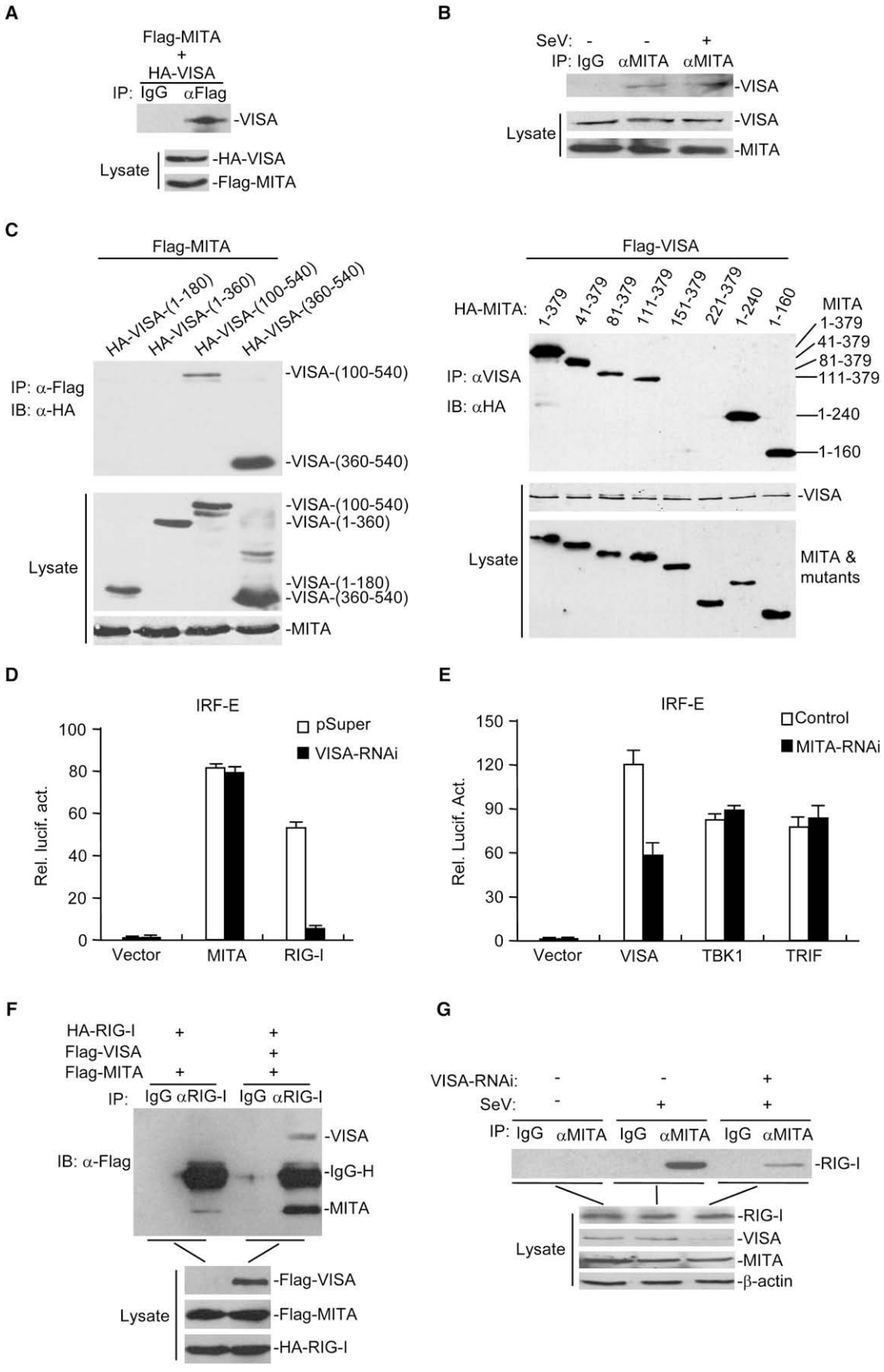
A
Flag-MITA
+
HA-VISA
IP: IgG αFlag
-VISA
Lysate
-HA-VISA
-Flag-MITA
B
SeV: - - +
IP: IgG αMITA αMITA
-VISA
Lysate
-VISA
-MITA
C
Flag-MITA
HA-VISA-(1-180)
HA-VISA-(1-360)
HA-VISA-(100-540)
HA-VISA-(360-540)
IP: α-Flag
IB: α-HA
-VISA-(100-540)
-VISA-(360-540)
Lysate
-VISA-(100-540)
-VISA-(1-360)
-VISA-(1-180)
-VISA-(360-540)
-MITA
Flag-VISA
HA-MITA: 1-379 41-379 81-379 111-379 151-379 221-379 1-240 1-160
MITA
1-379
41-379
81-379
111-379
1-240
1-160
IP: αVISA
IB: αHA
-VISA
Lysate
MITA &
mutants
D
IRF-E
pSuper
VISA-RNAi
Rel. lucif. act.
100
80
60
40
20
0
Vector
MITA
RIG-I
E
IRF-E
Control
MITA-RNAi
Rel. Lucif. Act.
150
120
90
60
30
0
Vector
VISA
TBK1
TRIF
F
HA-RIG-I + +
Flag-VISA +
Flag-MITA + +
IP: IgG αRIG-I IgG αRIG-I
IB: α-Flag
-VISA
-IgG-H
-MITA
Lysate
-Flag-VISA
-Flag-MITA
-HA-RIG-I
G
VISA-RNAi: - - +
SeV: - + +
IP: IgG αMITA IgG αMITA IgG αMITA
-RIG-I
Lysate
-RIG-I
-VISA
-MITA
-β-actin

TBK1-Mediated Phosphorylation of MITA Is Critical for Virus-Triggered IRF3 Activation

During the coimmunoprecipitation experiments, we routinely observed that TBK1 but not its kinase-inactive mutant caused a shift of MITA to higher molecular weight bands (Figure 6C); such a shift was due to TBK1 phosphorylation because treatment with phosphatase diminished the shift (Figure 7A). We made a series of MITA mutants in which one or more potential phosphorylation residues predicted by the NetPhos program were mutated to alanines. Immunoblot analysis indicated that mutation of S324 and 326 or S358 to alanine reduced TBK1-mediated phosphorylation of MITA (Figure 7B). Interestingly, the MITA(S358A) mutant failed to activate IRF-E and acted as a dominant-negative mutant that dramatically inhibited SeV-induced IRF-E activation (Figure 7C). We further confirmed that S358 is a true phosphorylation site targeted by TBK1 by mass spectrometry analysis (Figure S12). Consistent with its inability to activate IRF-E, the mutation of S358 to alanine impaired the ability of MITA to interact with TBK1 and to enhance the interaction between TBK1 and IRF3 (Figure S13).

To determine whether MITA is a true phosphoprotein, we performed ^{32}P in vivo labeling experiments. The results indicated that MITA was basally phosphorylated and that its phosphorylation was enhanced after viral infection (Figure 7D). Cotransfection of a kinase-inactive TBK1 mutant inhibited virus-induced MITA phosphorylation. Mutation of the putative TBK1 target sites also reduced the phosphorylation of MITA in response to SeV infection (Figure 7E). Consistently, MITA activated IRF-E in wild-type but not *Tbk1*$^{-/-}$ mouse embryonic fibroblasts (MEFs), whereas ectopic expression of TBK1 restored the ability of MITA to activate IRF-E in *Tbk1*$^{-/-}$ cells (Figure 7F). Taken together, these data suggest that viral infection causes TBK1-mediated MITA phosphorylation, which is important for virus-triggered IRF3 activation.

DISCUSSION

Previous studies have demonstrated that the mitochondrial protein VISA plays an essential role in virus-triggered induction of type I IFNs and innate antiviral immunity. In this study, we identified MITA as a VISA-associated mitochondrial protein that functions downstream of VISA in the IRF3-activation pathway.

Similar to VISA, MITA is ubiquitously expressed in all examined human tissues, and such an expression is consistent with the notion that type I IFNs are rapidly induced by viruses in all cell types. Overexpression of MITA activated IRF3. Conversely, knockdown of endogenous MITA abolished virus-triggered activation of IRF3 and induction of *IFNB1* and other IRF3-dependent downstream genes. Consistently, overexpression of MITA inhibited viral replication, whereas knockdown of MITA had an opposite effect. These data demonstrate that MITA is a critical component in the virus-triggered IRF3-activation pathway and cellular antiviral response. Although overexpression of MITA did not activate NF-κB, knockdown of MITA inhibited virus-triggered NF-κB activation. This observation suggests a potential crosstalk between virus-triggered IRF3 and NF-κB activation pathways at the MITA level. In this context, it has been demonstrated that the IKK regulatory subunit NEMO(IKKγ) is required for virus-triggered IRF3 activation (Zhao et al., 2007). We attempted to investigate the mechanism that leads to MITA involvement in the virus-triggered NF-κB activation pathway. However, coimmunoprecipitation experiments failed to detect an interaction between MITA and downstream proteins known to be involved in virus-triggered NF-κB activation, including TRAF6, IKKα, IKKβ, IKKγ, TRADD, FADD, and RIP. How MITA is involved in virus-triggered NF-κB activation is currently unknown.

Structural analysis indicates that MITA contains four transmembrane regions but lacks a conserved N-terminal signal peptide or mitochondrial targeting sequence. Biochemical and immunofluorescent-staining experiments suggest that MITA is localized to the outer membrane of mitochondria and that the third transmembrane region is important for its mitochondrial localization. Interestingly, VISA also lacks a detectable N-terminal mitochondrial targeting sequence, and its mitochondrial localization requires its C-terminal transmembrane region (Seth et al., 2005). Coimmunoprecipitation experiments indicated that MITA was constitutively associated with VISA. Deletion analysis indicates that the C terminus of VISA (aa 360–540) and the region spanning the third and fourth transmembrane domains of MITA (aa 111–160) were required for their interaction and localization to the mitochondria. These observations suggest that MITA and VISA are constitutively localized to the outer membrane of mitochondria as a complex.

Figure 5. MITA Interacts with VISA and Is Recruited to RIG-I

(A) MITA interacts with VISA. 293 cells (2×10^6) were transfected with the indicated plasmids (8 μg each). Cell lysates were immunoprecipitated with anti-Flag or control IgG. The immunoprecipitates were analyzed by immunoblotting with anti-HA (top panel). The expression of the transfected proteins were analyzed by immunoblotting with anti-HA and anti-Flag (middle and bottom panels) respectively.

(B) MITA interacts with VISA in untransfected cells. 293 cells (1×10^8) were infected with SeV or left uninfected for 2 hr. Cells were lysed and immunoprecipitation and immunoblot analysis were performed with the indicated antibodies.

(C) Domain mapping of the VISA-MITA interaction. The experiments were performed similarly as in (A).

(D) VISA RNAi inhibits RIG-I- but not MITA-mediated IRF-E activation. 293 cells (1×10^5) were transfected with the indicated plasmids (1 μg each). Luciferase assays were performed 24 hr after transfection. Graphs show mean ± SD, n = 3.

(E) Knockdown of MITA inhibits VISA- but not TRIF- and TBK1-mediated signaling. 293 cells (1×10^5) were first transfected with a MITA RNAi or control plasmid (1 μg). One day later, cells were selected with puromycin (1 μg/ml) for 24 hr and then retransfected with IRF-E luciferase and the indicated expression plasmids (0.1 μg each). Luciferase assays were performed 24 hr after the second transfection. Graphs show mean ± SD, n = 3.

(F) VISA mediates the interaction between RIG-I and MITA. 293 cells (2×10^6) were transfected with the indicated plasmids (8 μg each). Twenty hours after transfection, immunoprecipitation and immunoblot analysis were performed with the indicated antibodies.

(G) MITA is associated with RIG-I through VISA. 293 cells were left untransfected or transfected with the VISA RNAi plasmid. The cells were then treated with SeV or left untreated for 2 hr before immunoprecipitation and immunoblot analysis were performed with the indicated antibodies.

For (A), (B), (C), (F), and (G), the experiments were repeated for three times with similar results.

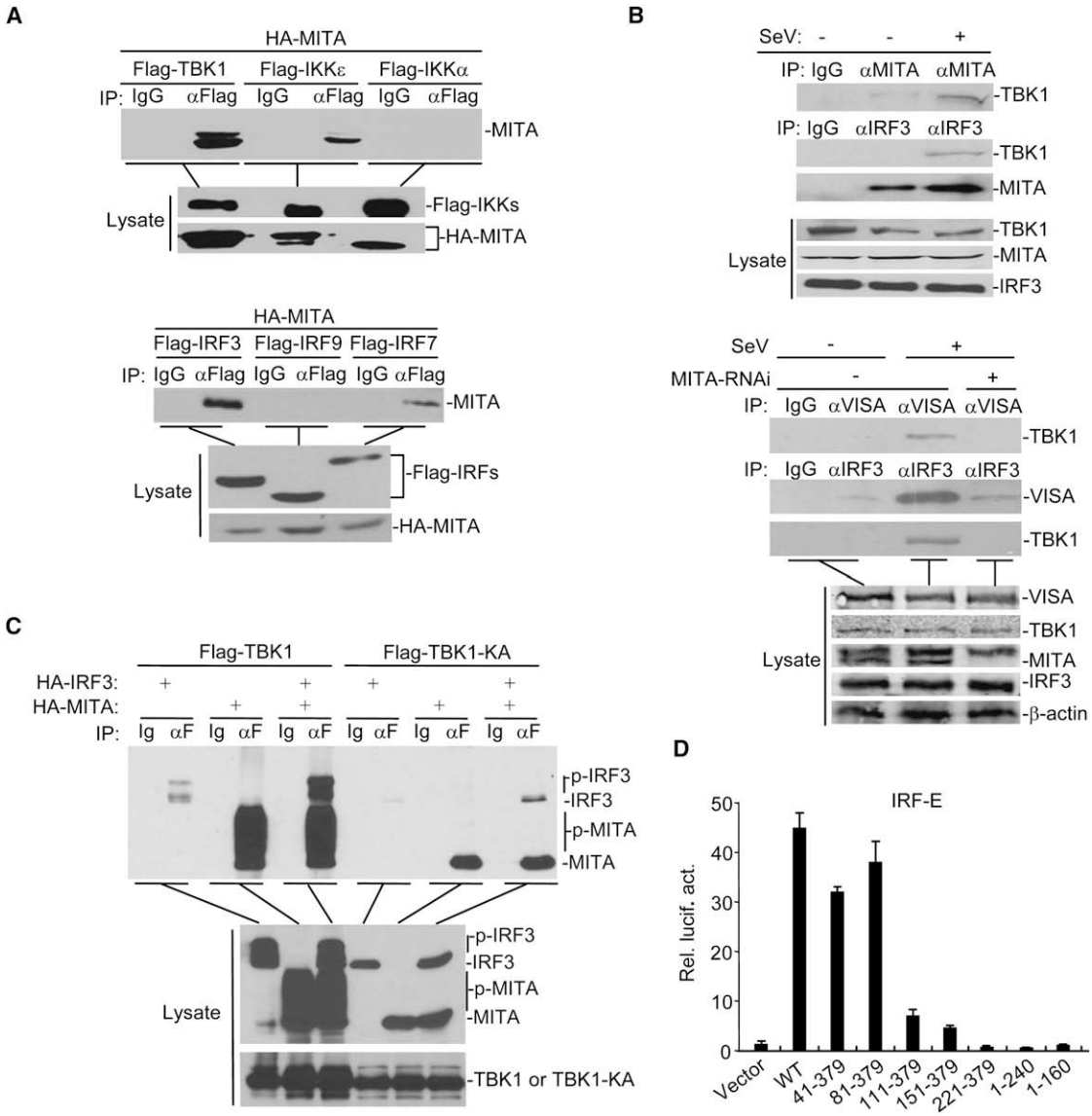

Figure 6. MITA Links IRF3 and TBK1 to the VISA-Associated Complex

(A) MITA interacts with TBK1, IKKε, and IRF3/7. 293 cells (2×10^6) were transfected with the indicated expression plasmids (8 μg each), and coimmunoprecipitation experiments were performed with the indicated antibodies.

(B) TBK1 and IRF3 are recruited to VISA through MITA after viral infection. Upper panels show endogenous association of MITA with TBK1 and IRF3. As shown in the lower panels, knockdown of MITA impairs viral-infection-induced recruitment of TBK1 and IRF3 to VISA. 293 cells (1×10^8) were untransfected (upper panels) or transfected with control or MITA RNAi plasmid (lower panels). Cells were infected with SeV or left untreated for 2 hr as indicated before coimmunoprecipitation experiments were performed.

(C) MITA enhances the interaction between TBK1 and IRF3. 293 cells (2×10^6) were transfected with the indicated plasmids (8 μg each). Immunoprecipitation and immunoblot analysis were performed with the indicated antibodies.

(D) Domain mapping of MITA-mediated IRF-E activation. Reporter assays were performed as in Figure 2B. Graphs show mean ± SD, n = 3.

For (A–C), the experiments were repeated for three times with similar results.

Several lines of experiments suggest that MITA acts downstream of VISA and represents the branching site for VISA-mediated IRF3-activation pathway. First, overexpression of VISA activated both NF-κB and IRF3, whereas MITA only activates IRF3. Second, knockdown of MITA inhibited VISA- but not TRIF- and TBK1-mediated IRF-E activation, whereas knockdown of VISA has no effects on MITA-mediated IRF-E activation. Third, MITA is associated with RIG-I in a viral-infection-dependent manner, and this association was diminished by knockdown of VISA.

Coimmunoprecipitation experiments indicated that IRF3 was constitutively associated with MITA, whereas TBK1 was recruited to MITA upon viral infection. In mammalian overexpression system, TBK1 interacted with IRF3 weakly and this interaction was dramatically enhanced by MITA. Both TBK1 and IRF3

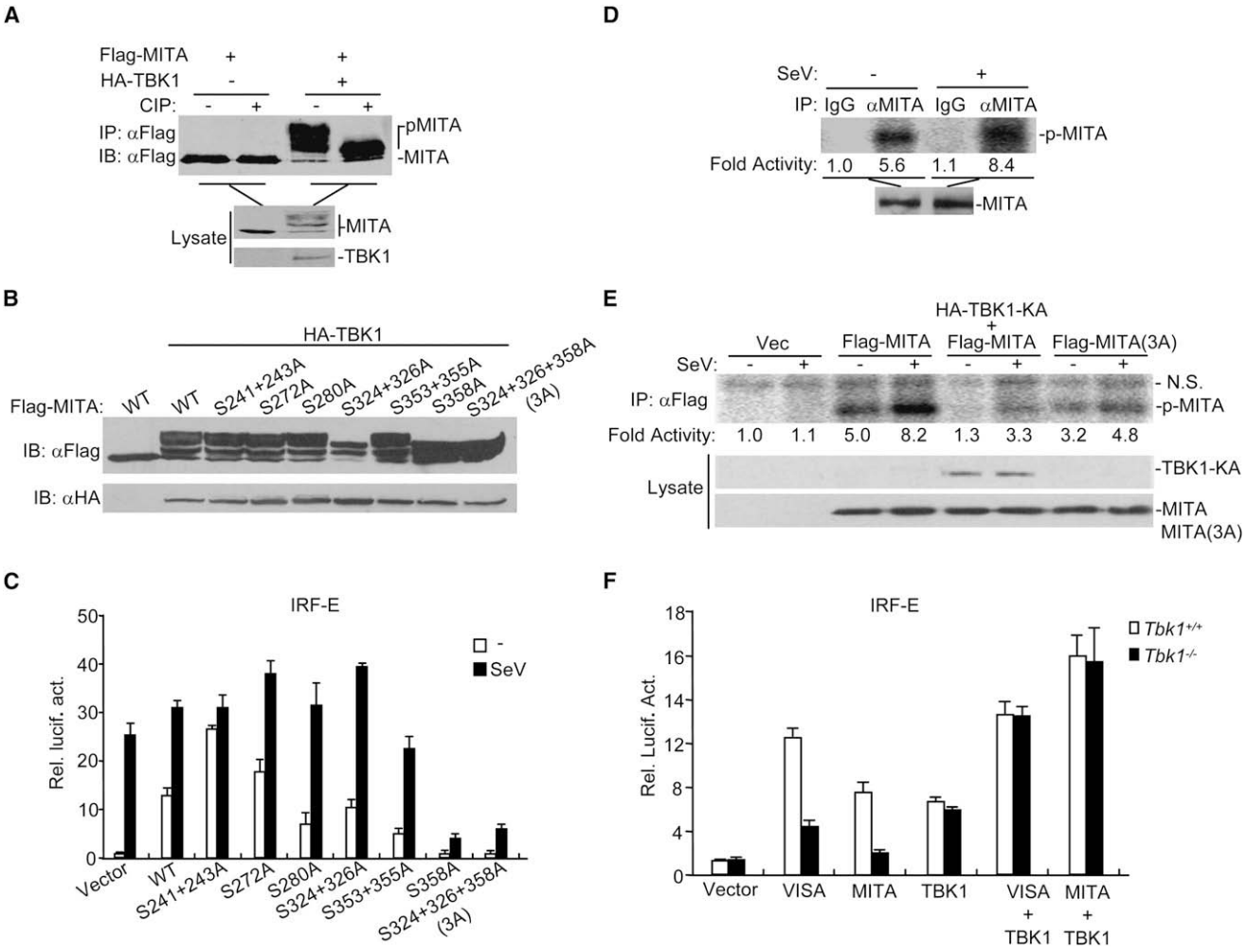

Figure 7. TBK1-Mediated Phosphorylation of MITA Is Critical for Virus-Triggered IRF3 Activation

(A) Phosphorylation of MITA by TBK1 is abolished by calf intestine phosphatase (CIP) treatment. 293 cells (2×10^6) were transfected with the indicated plasmids (8 μg each). Cell lysates were immunoprecipitated with anti-Flag. The immunoprecipitates were treated with buffer or CIP and analyzed by immunoblot with anti-Flag (upper panel). Expression of the transfected proteins were analyzed by immunoblots with anti-Flag (middle panel) or anti-HA (bottom panel).

(B) Mutation analysis of potential TBK1 phosphorylation sites. 293 cells were transfected with the indicated plasmids and immunoblot analysis was performed with the indicated antibodies.

(C) Effects of the MITA mutants on SeV-induced IRF-E activation. 293 cells (1×10^5) were transfected with the indicated plasmids (0.5 μg each). Twenty-four hours after transfection, cells were infected with SeV or left uninfected for 8 hr before luciferase assays were performed. Graphs show mean ± SD, n = 3.

(D) Endogenous MITA is phosphorylated in vivo. 293 cells (2×10^7) were treated with SeV or left untreated for 2 hr and then labeled with ^{32}P orthophosphate. The cell lysates were immunoprecipitated with anti-MITA antibody or control IgG. The immunoprecipitates were analyzed by SDS-PAGE and autoradiography (upper panel). The level of phosphorylation of MITA was quantitated by the Bio-Rad Quantity One program, and fold activity was shown. Expression of MITA protein was detected by immunoblot analysis (lower panel).

(E) Phosphorylation of MITA is blocked by TBK1-KA mutant. 293 cells (1×10^7) were transfected with the indicated expression plasmids (8 μg each) for 20 hr, treated with SeV or left untreated for 2 hr, and then labeled with ^{32}P orthophosphate. The cell lysates were immunoprecipitated with anti-Flag. The immunoprecipitates were analyzed and MITA phosphorylation was quantitated as in (D) (upper panel). Expression of transfected proteins was detected by immunoblot analysis with anti-HA (middle panel) or anti-Flag (lower panel).

(F) MITA activates IRF-E in wild-type but not *Tbk1*$^{-/-}$ mouse embryonic fibroblasts (MEFs). MEFs (1×10^5) were transfected with the indicated plasmids (1 μg each) and IRF-E reporter plasmids (0.2 μg). Reporter assays were performed 24 hr after transfection. Graphs show mean ± SD, n = 3.

For (A), (B), (D), and (E), the experiments were repeated for three times with similar results.

were recruited to VISA in a viral-infection-dependent process. Because knockdown of MITA impaired the association of VISA with TBK1 and IRF3, it suggests that MITA acts as the link for the recruitment of TBK1 and IRF3 to the VISA complex. Collectively, these studies suggest that the mitochondrial-membrane-bound and VISA-associated MITA provides a scaffold for assembly of a complex activating the IRF3 arm of virus-triggered signaling. In our previous report (Xu et al., 2005) and the

current study, we found that VISA is associated with IRF3 in a viral-infection-dependent manner, whereas MITA interacts with VISA and IRF3 constitutively. The simplest explanation for these observations is that two distinct complexes exist on the mitochondrial membrane under physiological conditions: the VISA-MITA and MITA-IRF3 complexes. After viral infection, these two complexes may be brought together by MITA-MITA interaction. In this context, we demonstrated that MITA can self-oligomerize.

MITA was phosphorylated by TBK1 and the phosphorylation was increased after viral infection. Ser358 of MITA was a critical target of TBK1 because the MITA(S358A) mutant failed to activate IRF-E and acted as a dominant-negative mutant to inhibit SeV-induced IRF-E activation. Consistently, MITA(S358A) also lost its ability to interact with TBK1 and to enhance the interaction between TBK1 and IRF3. The simplest explanation for these observations is that upon viral infection, TBK1 is recruited to the VISA-MITA-IRF3 complex, in which TBK1 first phosphorylates MITA, a step required for its subsequent phosphorylation of IRF3. Consistently, MITA activates IRF-E in wild-type but not *Tbk1*$^{-/-}$ mouse embryonic fibroblasts.

In our experiments, we found that mutation of the three serine residues to alanine (MITA3A) did not completely abolish the phosphorylation of MITA by TBK1. In addition, phosphorylation of MITA3A mutant was still increased after viral infection, although to a much lower degree in comparison to wild MITA. The simplest explanation for this observation is that additional TBK1 phosphorylation sites exist in MITA.

Various studies have indicated that TBK1 is a ubiquitously expressed kinase that is required for virus-triggered induction of type I IFNs. In contrast, expression of IKKε is limited to certain immune cells and is undetectable in most other cell types under physiological conditions (Akira et al., 2006; Honda et al., 2006; Huang et al., 2005; Lin et al., 2006a; Meylan et al., 2005). It has been suggested that IKKε is induced by viral infection and that the induced IKKε functions in a redundant role to its ubiquitous counterpart, TBK1, in the activation of IRF3 and IRF7. Gene-deletion studies have confirmed that IKKε is not required for virus-triggered induction of type I IFNs, but is required for type I IFN-induced activation of STAT1 and induction of a subset of type I IFN-stimulated genes (Hemmi et al., 2004; Perry et al., 2004; Tenoever et al., 2007). Similarly, IRF3 is ubiquitously expressed, whereas IRF7 is induced after viral infection. Therefore, in most cell types, both IKKε and IRF7 are not required for the first wave of induction of type I IFNs but are involved in the amplification of type I IFNs after viral infection. Because of these reasons, we performed detailed studies on the relationship between MITA and TBK1-IRF3 but not IKKε-IRF7. Nevertheless, we found MITA could interact with IKKε and IRF7 and promote IKKε-IRF3 interaction. These studies suggest that MITA can act as a scaffold for IKKε and IRF7 in similar ways as for TBK1 and IRF3 and is probably important for the amplification of type I IFN induction after viral infection.

On the basis of our findings, we propose a working model on the role of MITA in virus-triggered signaling. In this model, viral RNA is recognized by RIG-I and MDA5, which then interact with the mitochondrial protein VISA. VISA signals IKK-NF-κB activation through TRAF6 or TRAFDD-FADD-RIP. Concurrently, VISA interacts with the mitochondrial protein MITA, which interacts with IRF3 and recruits TBK1 upon viral infection. Previously, studies have demonstrated a role for TRAF3 in VISA-mediated IRF3 activation (Oganesyan et al., 2006; Saha et al., 2006). In this context, we found that MITA is able to interact with TRAF3. How TRAF3 is involved in MITA-mediated IRF3 activation is unknown at this time. Once recruited to the VISA-associated complex, TBK1 phosphorylates MITA and this step may be important for subsequent phosphorylation of IRF3 by TBK1. Various studies suggest that virus-triggered type I IFN signaling pathways are also positively regulated by TRIM25-mediated ubiquitation of RIG-I (Gack et al., 2007) or negatively regulated by a divergent groups of cellular or viral proteins, such as A20 (Lin et al., 2006b), DUBA (Kayagaki et al., 2007), RNF125 (Arimoto et al., 2007), LGP2 (Yoneyama et al., 2005), NLRX1 (Moore et al., 2008), DAK (Diao et al., 2007), SIKE (Huang et al., 2005), Pin1(Saitoh et al., 2006), V proteins (Andrejeva et al., 2004), and NS3/4A (Meylan et al., 2005). The identification of MITA as a critical mediator of virus-triggered IRF3 activation and type I IFN expression contributes to the elucidation of the complicated molecular mechanisms of cellular antiviral response and further demonstrates the importance of certain mitochondrial proteins in innate antiviral immunity.

EXPERIMENTAL PROCEDURES

Expression Cloning

Expression cloning was performed similarly as described (Kawai et al., 2005). In brief, a human spleen cDNA library (Stratagene) was divided into ~150 clones per pool and the plasmid DNA was prepared for IRF-E luciferase reporter assay with 293 cells. The positive pools were further divided into subpools of ~10 clones, which were tested for their ability to activate IRF-E in reporter assays. Single clones were isolated from the positive subpools and again tested for their ability to activate IRF-E in reporter assays. The positive clones were sequenced and identified by BLAST searches of the GenBank databases.

Reagents

TNFα and IL-1β (R&D Systems); mouse monoclonal antibodies against Flag, HA and β-actin (Sigma), TBK1 (Imgenex), AIF, KDEL, Caspase3, COX4, and H2B (Santa Cruz Biotechnology); rabbit polyclonal antibodies against IRF3 (Santa Cruz Biotechnology); and phospho-IRF3 (Ser396) (Upstate) were purchased from the indicated manufacturers. SeV, VSV, and rabbit anti-VISA and RIG-I antibodies were previously described (Diao et al., 2007; Huang et al., 2005; Xu et al., 2005). Huh7 cells (D.-Y. Guo), *Tbk*$^{-/-}$ and wild-type MEFs (W. Yeh) and pEGFP-C3 (Y. Wu) were provided by the indicated investigators. Mouse and rabbit anti-MITA antisera were raised against recombinant human MITA (221~379) and MITA (161~379), respectively.

Constructs

NF-κB, IRF-E/ISRE, and the IFN-β promoter luciferase reporter plasmids, VISA RNAi plasmid, mammalian expression plasmids for HA- or Flag-tagged VISA and its mutants RIG-I, TBK1, IKKε, IKKα, IRF3, IRF7, IRF9, IRF3-DN, IRF7-DN, TRAF3, IKKε-KA, and TBK1-KA were previously described (Diao et al., 2007; Huang et al., 2005; Xu et al., 2005). Mammalian expression plasmids for human HA-, Flag- or GFP-tagged MITA and its truncated mutants were constructed by standard molecular biology techniques.

Transfection and Reporter Gene Assays

The 293 cells (~1 × 10^5) were seeded on 24-well dishes and transfected the following day by standard calcium phosphate precipitation. In the same experiment, we added empty control plasmid to ensure that each transfection receives the same amount of total DNA. To normalize for transfection efficiency, we added 0.01 μg of pRL-TK *Renilla* luciferase reporter plasmid to each

transfection. Luciferase assays were performed with a dual-specific luciferse assay kit (Promega). Firefly luciferase activities were normalized on the basis of *Renilla* luciferase activities. All reporter assays were repeated for at least three times. Data shown were average values ± SD from one representative experiment.

Coimmunoprecipitation, Immunoblot Analysis, Native PAGE, RNA Blot Analysis, and VSV Plaque Assays

These experiments were performed as described (Diao et al., 2007; Huang et al., 2005; Xu et al., 2005).

RNAi

The RNAi plasmids targeting human MITA mRNA were purchased from Origene. The target sequences were as following: MITA RNAi #1: 5′-gcaacagca tctatgagcttctggagaac-3′; #2: 5′-gtgcagtgagccagcggctgtatattctc;-3′ #3: 5′-gct ggcatggtcatattacatcggatatc-3′.

RT-PCR

RT-PCR was performed as described (Huang et al., 2005). Gene-specific primer sequences for *IFN-β* and *GAPDH* were as described (Huang et al., 2005) or were as follows: *ISG56*, forward: 5′-acggctgcctaatttacagc-3′, and reverse: 5′-agtggctgatatctgggtgc-3′; *ISG15*, forward: 5′-atgggctgggacctga cgg-3′, and reverse: 5′-ttagctccgcccgccaggct-3′.

Subcellular Fractionation

The 293 cells (5×10^7) infected with SeV or left uninfected for 2 hr were washed with PBS and lysed by douncing for 20 times in 2 ml homogenization buffer (10 mM Tris-HCl [pH 7.4], 2 mM MgCl2, 10 mM KCl, and 250 mM sucrose). The homogenate was centrifuged at 500 g for 10 min, and the pellet (P5) was saved as crude nuclei. The supernatant (S5) was centrifuged at 5000 g for 10 min to precipitate crude mitochondria (P5K). The supernatant (S5K) was further centrifuged at 50,000 g for 60 min for S50K and P50K generation.

Immunofluorescent Confocal Microscopy

The transfected 293 cells were incubated with the MitoTracker Red (Molecular Probes) for 30 min. The cells were then fixed with 4% paraformaldehyde for 10 min and observed with a Leica confocal microscope under a ×100 oil objective.

^{32}P In Vivo Labeling

Cells were infected with SeV or left untreated for 2 hr and then starved in phosphate-free DMEM/1% dialyzed FBS for 1 hr. Afterward, the cells were collected and labeled with ^{32}P orthophosphate (Perkin Elmer) at a concentration of 1 mCi/ml for 1 hr. The cells were then lysed and the lysates were immunoprecipitated with the indicated antibodies. The immunoprecipitates were analyzed by SDS-PAGE and autoradiography. Before labeling, we took a small fraction of cells for immunoblot analysis to detect protein expression.

SUPPLEMENTAL DATA

Supplemental Data include thirteen figures and can be found with this article online at http://www.immunity.com/cgi/content/full/29/4/538/DC1/.

ACKNOWLEDGMENTS

We thank L.-G. Xu, L. Guo, F. Yang, P. Xue, and R.-P. Wang for technique help, W.-C. Yeh, D.-Y. Guo, and Y. Wu for reagents. This work was supported by grants from the Chinese 973 program (#2006CB504301 and #2009CB522506), the National Natural Science Foundation of China (#30630019 and #30700431), and the Chinese 863 program (#2006AA02A306).

Received: May 29, 2008
Revised: September 2, 2008
Accepted: September 10, 2008
Published online: September 25, 2008

REFERENCES

Akira, S., Uematsu, S., and Takeuchi, O. (2006). Pathogen recognition and innate immunity. Cell *124*, 783–801.

Alexopoulou, L., Holt, A.C., Medzhitov, R., and Flavell, R.A. (2001). Recognition of double-stranded RNA and activation of NF-kappaB by Toll-like receptor 3. Nature *413*, 732–738.

Andrejeva, J., Childs, K.S., Young, D.F., Carlos, T.S., Stock, N., Goodbourn, S., and Randall, R.E. (2004). The V proteins of paramyxoviruses bind the IFN-inducible RNA helicase, mda-5, and inhibit its activation of the IFN-beta promoter. Proc. Natl. Acad. Sci. USA *101*, 17264–17269.

Arimoto, K., Takahashi, H., Hishiki, T., Konishi, H., Fujita, T., and Shimotohno, K. (2007). Negative regulation of the RIG-I signaling by the ubiquitin ligase RNF125. Proc. Natl. Acad. Sci. USA *104*, 7500–7505.

Diao, F., Li, S., Tian, Y., Zhang, M., Xu, L.G., Zhang, Y., Wang, R.P., Chen, D., Zhai, Z., Zhong, B., et al. (2007). Negative regulation of MDA5- but not RIG-I-mediated innate antiviral signaling by the dihydroxyacetone kinase. Proc. Natl. Acad. Sci. USA *104*, 11706–11711.

Durbin, J.E., Fernandez-Sesma, A., Lee, C.K., Rao, T.D., Frey, A.B., Moran, T.M., Vukmanovic, S., Garcia-Sastre, A., and Levy, D.E. (2000). Type I IFN modulates innate and specific antiviral immunity. J. Immunol. *164*, 4220–4228.

Fitzgerald, K.A., McWhirter, S.M., Faia, K.L., Rowe, D.C., Latz, E., Golenbock, D.T., Coyle, A.J., Liao, S.M., and Maniatis, T. (2003). IKKepsilon and TBK1 are essential components of the IRF3 signaling pathway. Nat. Immunol. *4*, 491–496.

Gack, M.U., Shin, Y.C., Joo, C.H., Urano, T., Liang, C., Sun, L., Takeuchi, O., Akira, S., Chen, Z., Inoue, S., and Jung, J.U. (2007). TRIM25 RING-finger E3 ubiquitin ligase is essential for RIG-I-mediated antiviral activity. Nature *446*, 916–920.

Han, K.J., Su, X., Xu, L.G., Bin, L.H., Zhang, J., and Shu, H.B. (2004). Mechanisms of the TRIF-induced interferon-stimulated response element and NF-kappaB activation and apoptosis pathways. J. Biol. Chem. *279*, 15652–15661.

Hemmi, H., Takeuchi, O., Sato, S., Yamamoto, M., Kaisho, T., Sanjo, H., Kawai, T., Hoshino, K., Takeda, K., and Akira, S. (2004). The roles of two IkappaB kinase-related kinases in lipopolysaccharide and double stranded RNA signaling and viral infection. J. Exp. Med. *199*, 1641–1650.

Hiscott, J. (2007). Convergence of the NF-kappaB and IRF pathways in the regulation of the innate antiviral response. Cytokine Growth Factor Rev. *18*, 483–490.

Honda, K., Takaoka, A., and Taniguchi, T. (2006). Type I interferon [corrected] gene induction by the interferon regulatory factor family of transcription factors. Immunity *25*, 349–360.

Hornung, V., Ellegast, J., Kim, S., Brzozka, K., Jung, A., Kato, H., Poeck, H., Akira, S., Conzelmann, K.K., Schlee, M., et al. (2006). 5′-Triphosphate RNA is the ligand for RIG-I. Science *314*, 994–997.

Huang, J., Liu, T., Xu, L.G., Chen, D., Zhai, Z., and Shu, H.B. (2005). SIKE is an IKK epsilon/TBK1-associated suppressor of TLR3- and virus-triggered IRF-3 activation pathways. EMBO J. *24*, 4018–4028.

Kato, H., Takeuchi, O., Sato, S., Yoneyama, M., Yamamoto, M., Matsui, K., Uematsu, S., Jung, A., Kawai, T., Ishii, K.J., et al. (2006). Differential roles of MDA5 and RIG-I helicases in the recognition of RNA viruses. Nature *441*, 101–105.

Katze, M.G., He, Y., and Gale, M., Jr. (2002). Viruses and interferon: A fight for supremacy. Nat. Rev. Immunol. *2*, 675–687.

Kawai, T., Takahashi, K., Sato, S., Coban, C., Kumar, H., Kato, H., Ishii, K.J., Takeuchi, O., and Akira, S. (2005). IPS-1, an adaptor triggering RIG-I- and Mda5-mediated type I interferon induction. Nat. Immunol. *6*, 981–988.

Kayagaki, N., Phung, Q., Chan, S., Chaudhari, R., Quan, C., O'Rourke, K.M., Eby, M., Pietras, E., Cheng, G., Bazan, J.F., et al. (2007). DUBA: A deubiquitinase that regulates type I interferon production. Science *318*, 1628–1632.

Kumar, H., Kawai, T., Kato, H., Sato, S., Takahashi, K., Coban, C., Yamamoto, M., Uematsu, S., Ishii, K.J., Takeuchi, O., and Akira, S. (2006). Essential role of IPS-1 in innate immune responses against RNA viruses. J. Exp. Med. *203*, 1795–1803.

Levy, D.E., and Garcia-Sastre, A. (2001). The virus battles: IFN induction of the antiviral state and mechanisms of viral evasion. Cytokine Growth Factor Rev. *12*, 143–156.

Levy, D.E., and Marie, I.J. (2004). RIGging an antiviral defense–it's in the CARDs. Nat. Immunol. *5*, 699–701.

Lin, R., Lacoste, J., Nakhaei, P., Sun, Q., Yang, L., Paz, S., Wilkinson, P., Julkunen, I., Vitour, D., Meurs, E., and Hiscott, J. (2006a). Dissociation of a MAVS/IPS-1/VISA/Cardif-IKKepsilon molecular complex from the mitochondrial outer membrane by hepatitis C virus NS3–4A proteolytic cleavage. J. Virol. *80*, 6072–6083.

Lin, R., Yang, L., Nakhaei, P., Sun, Q., Sharif-Askari, E., Julkunen, I., and Hiscott, J. (2006b). Negative regulation of the retinoic acid-inducible gene I-induced antiviral state by the ubiquitin-editing protein A20. J. Biol. Chem. *281*, 2095–2103.

Maniatis, T., Falvo, J.V., Kim, T.H., Kim, T.K., Lin, C.H., Parekh, B.S., and Wathelet, M.G. (1998). Structure and function of the interferon-beta enhanceosome. Cold Spring Harb. Symp. Quant. Biol. *63*, 609–620.

Matsui, K., Kumagai, Y., Kato, H., Sato, S., Kawagoe, T., Uematsu, S., Takeuchi, O., and Akira, S. (2006). Cutting edge: Role of TANK-binding kinase 1 and inducible IkappaB kinase in IFN responses against viruses in innate immune cells. J. Immunol. *177*, 5785–5789.

Meylan, E., Curran, J., Hofmann, K., Moradpour, D., Binder, M., Bartenschlager, R., and Tschopp, J. (2005). Cardif is an adaptor protein in the RIG-I antiviral pathway and is targeted by hepatitis C virus. Nature *437*, 1167–1172.

Michallet, M.C., Meylan, E., Ermolaeva, M.A., Vazquez, J., Rebsamen, M., Curran, J., Poeck, H., Bscheider, M., Hartmann, G., Konig, M., et al. (2008). TRADD protein is an essential component of the RIG-like helicase antiviral pathway. Immunity *28*, 651–661.

Moore, C.B., Bergstralh, D.T., Duncan, J.A., Lei, Y., Morrison, T.E., Zimmermann, A.G., Accavitti-Loper, M.A., Madden, V.J., Sun, L., Ye, Z., et al. (2008). NLRX1 is a regulator of mitochondrial antiviral immunity. Nature *451*, 573–577.

Nakaya, T., Sato, M., Hata, N., Asagiri, M., Suemori, H., Noguchi, S., Tanaka, N., and Taniguchi, T. (2001). Gene induction pathways mediated by distinct IRFs during viral infection. Biochem. Biophys. Res. Commun. *283*, 1150–1156.

Navarro, L., Mowen, K., Rodems, S., Weaver, B., Reich, N., Spector, D., and David, M. (1998). Cytomegalovirus activates interferon immediate-early response gene expression and an interferon regulatory factor 3-containing interferon-stimulated response element-binding complex. Mol. Cell. Biol. *18*, 3796–3802.

Oganesyan, G., Saha, S.K., Guo, B., He, J.Q., Shahangian, A., Zarnegar, B., Perry, A., and Cheng, G. (2006). Critical role of TRAF3 in the Toll-like receptor-dependent and -independent antiviral response. Nature *439*, 208–211.

Oshiumi, H., Matsumoto, M., Funami, K., Akazawa, T., and Seya, T. (2003). TICAM-1, an adaptor molecule that participates in Toll-like receptor 3-mediated interferon-beta induction. Nat. Immunol. *4*, 161–167.

Perry, A.K., Chow, E.K., Goodnough, J.B., Yeh, W.C., and Cheng, G. (2004). Differential requirement for TANK-binding kinase-1 in type I interferon responses to toll-like receptor activation and viral infection. J. Exp. Med. *199*, 1651–1658.

Pichlmair, A., Schulz, O., Tan, C.P., Naslund, T.I., Liljestrom, P., Weber, F., and Reis e Sousa, C. (2006). RIG-I-mediated antiviral responses to single-stranded RNA bearing 5′-phosphates. Science *314*, 997–1001.

Saha, S.K., Pietras, E.M., He, J.Q., Kang, J.R., Liu, S.Y., Oganesyan, G., Shahangian, A., Zarnegar, B., Shiba, T.L., Wang, Y., and Cheng, G. (2006). Regulation of antiviral responses by a direct and specific interaction between TRAF3 and Cardif. EMBO J. *25*, 3257–3263.

Saitoh, T., Tun-Kyi, A., Ryo, A., Yamamoto, M., Finn, G., Fujita, T., Akira, S., Yamamoto, N., Lu, K.P., and Yamaoka, S. (2006). Negative regulation of interferon-regulatory factor 3-dependent innate antiviral response by the prolyl isomerase Pin1. Nat. Immunol. *7*, 598–605.

Seth, R.B., Sun, L., Ea, C.K., and Chen, Z.J. (2005). Identification and characterization of MAVS, a mitochondrial antiviral signaling protein that activates NF-kappaB and IRF 3. Cell *122*, 669–682.

Sun, Q., Sun, L., Liu, H.H., Chen, X., Seth, R.B., Forman, J., and Chen, Z.J. (2006). The specific and essential role of MAVS in antiviral innate immune responses. Immunity *24*, 633–642.

Tenoever, B.R., Ng, S.L., Chua, M.A., McWhirter, S.M., Garcia-Sastre, A., and Maniatis, T. (2007). Multiple functions of the IKK-related kinase IKKepsilon in interferon-mediated antiviral immunity. Science *315*, 1274–1278.

Wathelet, M.G., Clauss, I.M., Nols, C.B., Content, J., and Huez, G.A. (1987). New inducers revealed by the promoter sequence analysis of two interferon-activated human genes. Eur. J. Biochem. *169*, 313–321.

Wathelet, M.G., Lin, C.H., Parekh, B.S., Ronco, L.V., Howley, P.M., and Maniatis, T. (1998). Virus infection induces the assembly of coordinately activated transcription factors on the IFN-beta enhancer in vivo. Mol. Cell *1*, 507–518.

Xu, L.G., Wang, Y.Y., Han, K.J., Li, L.Y., Zhai, Z., and Shu, H.B. (2005). VISA is an adapter protein required for virus-triggered IFN-beta signaling. Mol. Cell *19*, 727–740.

Yamamoto, M., Sato, S., Hemmi, H., Hoshino, K., Kaisho, T., Sanjo, H., Takeuchi, O., Sugiyama, M., Okabe, M., Takeda, K., and Akira, S. (2003). Role of adaptor TRIF in the MyD88-independent toll-like receptor signaling pathway. Science *301*, 640–643.

Yamamoto, M., Sato, S., Mori, K., Hoshino, K., Takeuchi, O., Takeda, K., and Akira, S. (2002). Cutting edge: A novel Toll/IL-1 receptor domain-containing adapter that preferentially activates the IFN-beta promoter in the Toll-like receptor signaling. J. Immunol. *169*, 6668–6672.

Yoneyama, M., Kikuchi, M., Matsumoto, K., Imaizumi, T., Miyagishi, M., Taira, K., Foy, E., Loo, Y.M., Gale, M., Jr., Akira, S., et al. (2005). Shared and unique functions of the DExD/H-box helicases RIG-I, MDA5, and LGP2 in antiviral innate immunity. J. Immunol. *175*, 2851–2858.

Yoneyama, M., Kikuchi, M., Natsukawa, T., Shinobu, N., Imaizumi, T., Miyagishi, M., Taira, K., Akira, S., and Fujita, T. (2004). The RNA helicase RIG-I has an essential function in double-stranded RNA-induced innate antiviral responses. Nat. Immunol. *5*, 730–737.

Zhao, T., Yang, L., Sun, Q., Arguello, M., Ballard, D.W., Hiscott, J., and Lin, R. (2007). The NEMO adaptor bridges the nuclear factor-kappaB and interferon regulatory factor signaling pathways. Nat. Immunol. *8*, 592–600.